High spin resonances in the $\pi^+\pi^-\pi^-$ and $\pi^-\pi^0\pi^0$ systems at VES setup

Igor Kachaev, Dmitry Ryabchikov
for VES group, Protvino, Russia

Institute for High Energy Physics, Protvino.
E-mail Igor.Katchaev@ihep.ru

MESON 2018
Krakow, Poland
8 June 2018

Preface

Plan of the report

- Raw data.
- Two PWA methods
    - PWA with unlimited rank density matrix
    - PWA with rank 1 density matrix
- Comparison of the largest waves
- Waves for $J^P = 3^+$
- Waves for $J^P = 4^+$
- Conclusions

Raw data

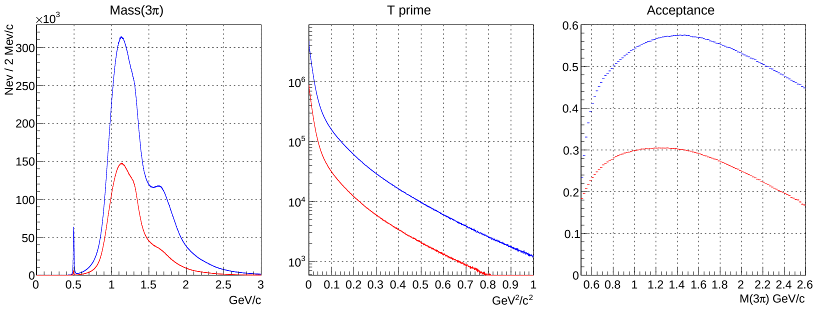

- We have full featured magnetic spectrometer with 29 GeV/c π^- beam, Be target, $|t'| = 0 \ldots 1\ GeV^2/c^2$
- Two final states $\pi^+ 2\pi^-$ and $\pi^- 2\pi^0$
  - $33 \cdot 10^6$ events in $\pi^-\pi^0\pi^0$ (leading statistics in the world)
  - $87 \cdot 10^6$ events in $\pi^+\pi^-\pi^-$ (leading statistics in the world)
- Here and below: blue line - $\pi^+\pi^-\pi^-$ red line - $\pi^-\pi^0\pi^0$

PWA methods. Partial waves

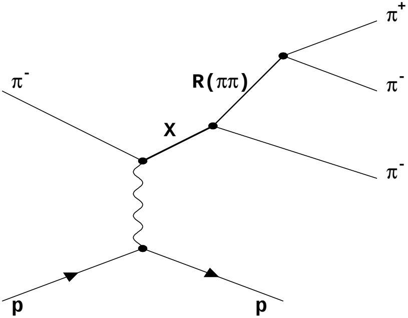

PWA amplitudes are constructed using isobar model, sequential decay via $\pi\pi$ subsystem. Wave has quantum numbers $J^P LM^\eta \mathrm{R}$ where J^P is spin-parity for 3π system, M^η is its projection of spin and naturality, R is the known resonance in $\pi\pi$ system, L is orbital momentum in $\mathrm{R}\pi$ decay. For all 3π charged states $I^G = 1^-$.

PWA methods. Common part

- Amplitudes are non relativistic (in GJ frame)
- Resonanses are relativistic Breit-Wigners
  $R = f_0(980),\ \varepsilon(1300),\ f_0(1500),\ \rho(770),\ f_2(1270),\ \rho_3(1690)$
  To describe $\pi\pi$ S-wave we use modified Au, Morgan, Pennnington M-solution with $f_0(980)$ withdrawn. We name it $\varepsilon(1300)$
- If we neglect phase space factors, due to GJ coefficients

$$R = \frac{\sigma(\pi^-\pi^0\pi^0)}{\sigma(\pi^+\pi^-\pi^-)} = \begin{cases} 1 & \text{for waves with } \rho(770),\ \rho_3(1690) \\ 1/2 & \text{for waves with } f_0(...),\ f_2(1270) \end{cases}$$

  All waves in $\pi^- 2\pi^0$ coupled to $\pi^0\pi^0$ have factor $1/2$
  To simplify comparison, they are scaled 2x.
- Below we use blue line for $\pi^+\pi^-\pi^-$, red line for $\pi^-\pi^0\pi^0$

PWA methods. The difference

PWA with full rank density matrix

- Amplitudes use d-functions (Hansen, Illinois PWA)
- fit parameters are elements of positive definite density matrix. Small number of waves are 100% coherent with each other. This fit is named full matrix below.
- Coherent part of the density matrix is the largest part of the matrix which has rank 1 and behaves like vector of amplitudes. It corresponds to the largest eigenvalue of density matrix. Named LEV below.

PWA with rank one density matrix

- Amplitudes use tensors (Zemach)
- Fit parameters are coupling coefficients – this is the same as rank one matrix. This fit is named rank 1 below.

Wave $1^{+}S0^{+}\rho$ for $\pi^{+}2\pi^{-}$ and $\pi^{-}2\pi^{0}$

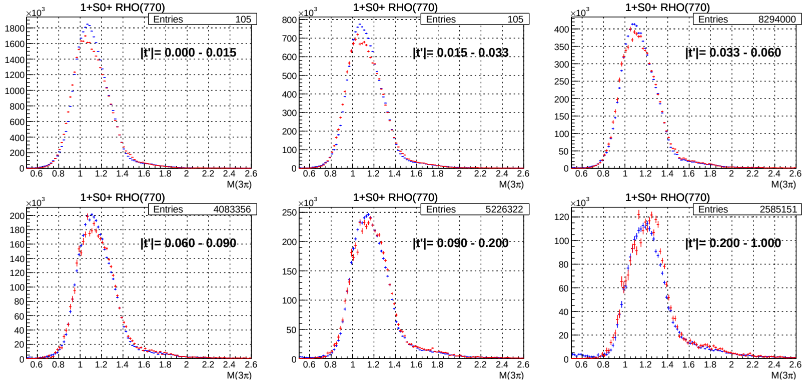

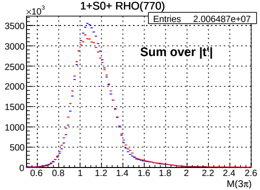

Blue $\pi^{+}2\pi^{-}$ red $\pi^{-}2\pi^{0}$

Systems are comparable without additional normalization in all $|t'|$ regions.

Largest waves in $\pi^+ 2\pi^-$ for full rank, LEV, rank 1

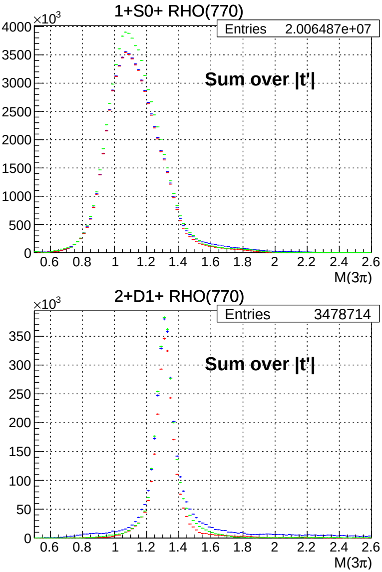

Full matrix — blue
LEV — red
rank 1 — green
Methods are comparable
without additional normalization.

Largest waves in $\pi^-2\pi^0$ for full rank, LEV, rank 1

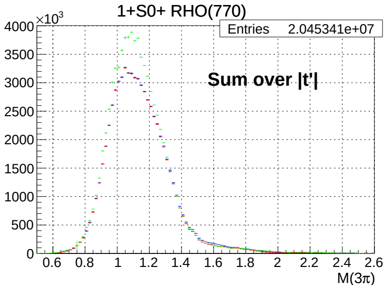

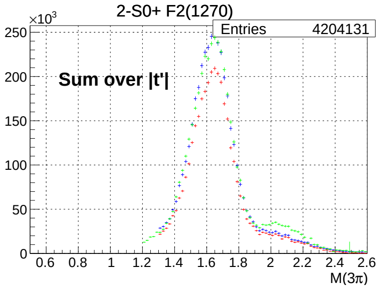

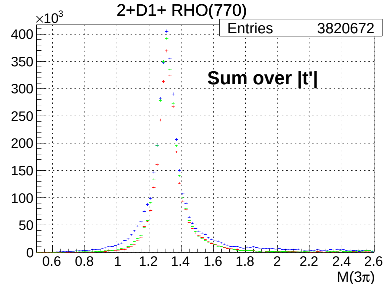

Full matrix — blue

LEV — red

rank 1 — green

Methods are comparable without additional normalization.

Waves 3^+ for $\pi^+2\pi^-$

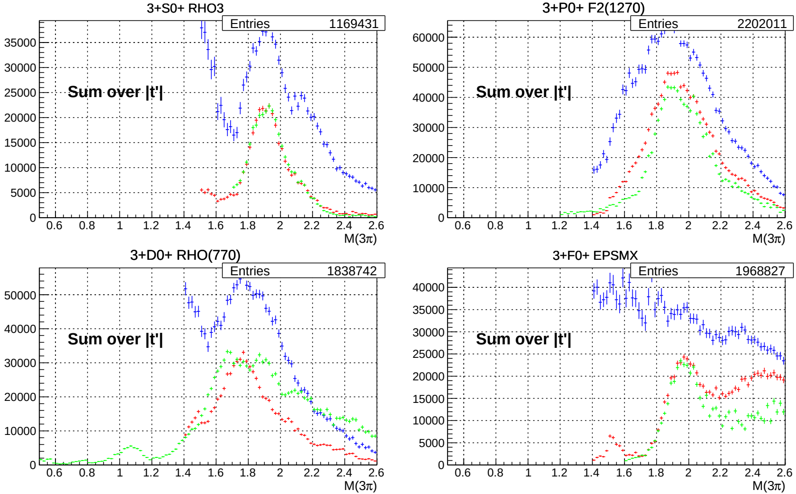

Clean resonant behavior is seen in $\rho_3\pi$ in all 3 methods. For $f_2\pi$ and $\rho\pi$ bumps are shapeless and shifted. For $\varepsilon\pi$ only coherent methods win; full density matrix contains garbage.

Waves 3^+ for $\pi^-2\pi^0$

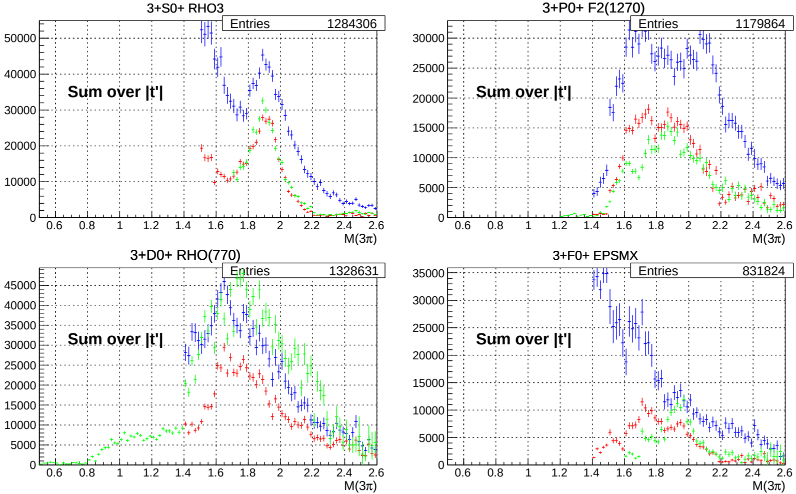

Clean resonant behavior is seen in $\rho_3\pi$ only, in all 3 methods. System $\pi^-2\pi^0$ suffers from 2x smaller acceptance and 2x smaller CG coefficient for $f_2\pi$ and $\varepsilon\pi$ waves.

Fits $3^+S0^+\rho_3$ for $\pi^+2\pi^-$, all t' ranges

Fit in 6 $|t'|$ ranges 0–0.015–0.033–0.060–0.090-0.200-1.000 GeV/c^2
Fit parameters are separate for all $|t'|$ bins. Fit is reasonably stable vrt $|t'|$.

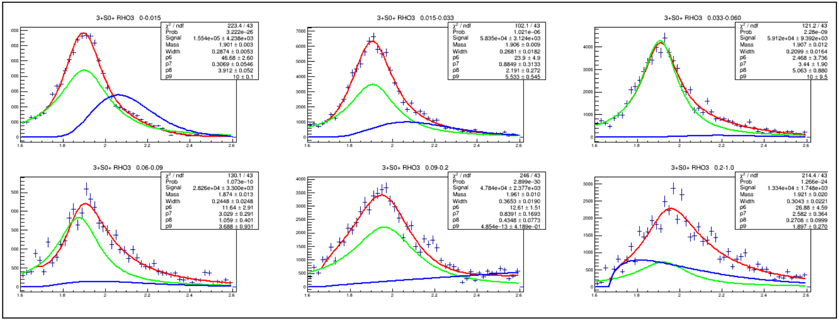

Green line — relativistic Breight-Wigner
Blue line — phase space background with exponential dumping
Red line — summary

Waves 4^+ for $\pi^+ 2\pi^-$

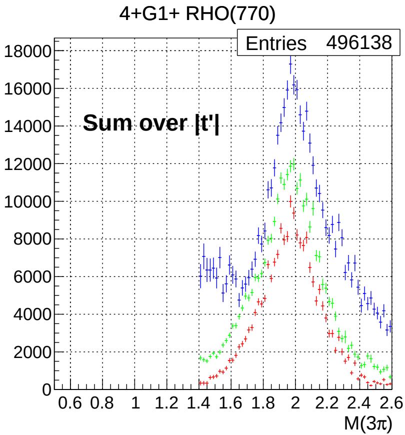

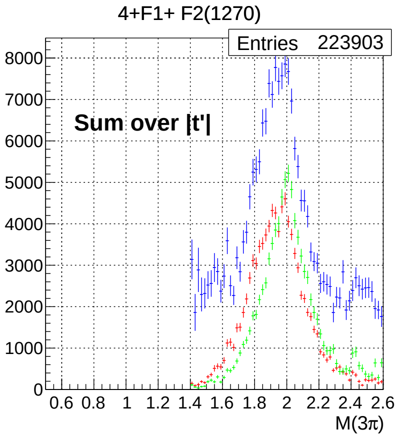

Resonant behavior is seen in both waves and all 3 methods.

Waves 4^+ for $\pi^-2\pi^0$

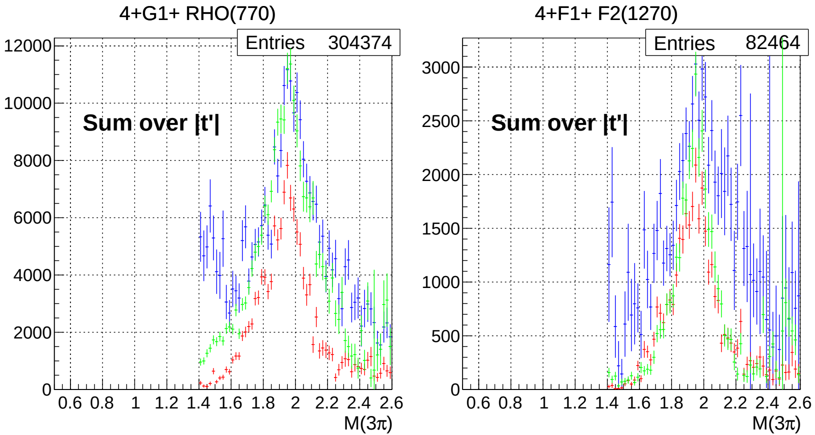

Resonant behavior is seen in both waves and all 3 methods.

Distribution over $|t'|$ for $4+$ waves for $\pi^+ 2\pi^-$

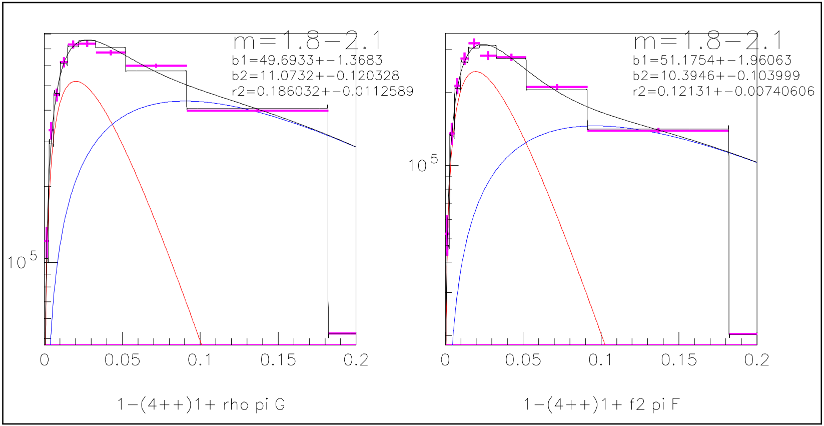

Special rank 1 fit with 10 t' ranges is done here.
Distributions over $|t|'$ for both 4^+ waves looks simular.
Gap at $|t'| = 0$ is expected for waves with $|M| = 1$.

Branching ratio $4^+G1^+\rho$ vs $4^+D1^+f_2$ for $\pi^+2\pi^-$ vs t'

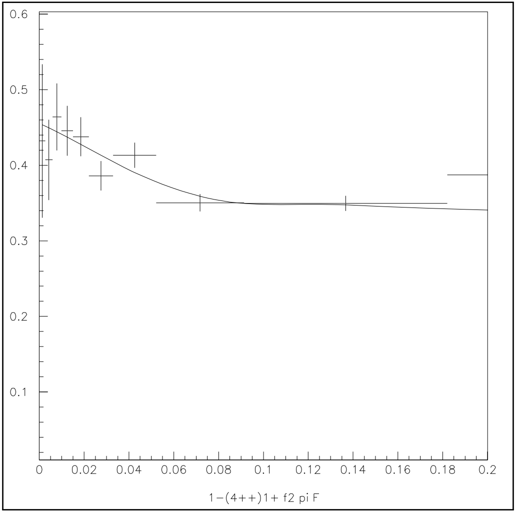

Branching ratio $f_2\pi_D$ vs $\rho\pi_G$ is stable with respect to $|t'|$

Conclusions

- Mass-independent PWA is done for $\pi^+\pi^-\pi^-$ and $\pi^-\pi^0\pi^0$ data with both unlimited rank and rank 1 PWA models. Results for for both systems and both methods coinside without additional normalization. The best coinsidence is between coherent part of density matrix and rank 1 results. Background looks suppressed in these methods w.r.t. full rank density matrix.
- Parameters of $a_3(1875)$ (PDG status — not confirmed) are measured. For $3^+S0^+\rho_3\pi$ in both $\pi^+\pi^-\pi^-$ and $\pi^-\pi^0\pi^0$

$$M = 1905 \pm 15\,\mathrm{GeV/c^2} \quad G = 250 \pm 30\,\mathrm{GeV/c^2}$$

No resonant behavior is found in $f_2\pi$ and $\rho\pi$ states. For $\varepsilon\pi$ state activity in coherent part of d.m. is seen in $\pi^+2\pi^-$ but not in $\pi^-2\pi^0$. State $\varepsilon\pi$ in $\pi^-2\pi^0$ suffers from 2x smaller acceptance and 2x smaller cross section due to CG coefficient.

Conclusions (cont'd)

- Decay of $a_4(2050)$ into $\pi^+\pi^-\pi^-$ and $\pi^-\pi^0\pi^0$ is seen. In $\rho\pi_G$ and $f_2\pi_F$ final states and both $\pi^+\pi^-\pi^-$ and $\pi^-\pi^0\pi^0$

$$M = 1980 \pm 10\,\mathrm{GeV/c^2} \quad G = 260 \pm 20\,\mathrm{GeV/c^2}$$

$$\frac{\sigma(a_4 \to f_2\pi_F)}{\sigma(a_4 \to \rho\pi_G)} = 0.50 \pm 0.05$$

Backup slides

Wave set used in the analysis

J^P	$J^P L M^\eta\ R$
FLAT	**FLAT**
$\mathbf{0^-}$	$0^-\mathrm{S}0^+\ \varepsilon$ $0^-\mathrm{S}0^+\ f_0$ $0^-\mathrm{S}0^+\ f_0(1500)$ $0^-\mathrm{P}0^+\ \rho$
$\mathbf{1^+}$	$1^+\mathrm{S}0^+\ \rho$ $1^+\mathrm{P}0^+\ \varepsilon$ $1^+\mathrm{D}0^+\ \rho$ $1^+\mathrm{P}0^+\ f_0$ $1^+\mathrm{P}0^+\ f_2$ $1^+\mathrm{S}1^+\ \rho$ $1^+\mathrm{P}1^+\ \varepsilon$ $1^+\mathrm{S}1^-\ \rho$
$\mathbf{1^-}$	$1^-\mathrm{P}1^+\ \rho$ $1^-\mathrm{P}0^-\ \rho$ $1^-\mathrm{P}1^-\ \rho$
$\mathbf{2^-}$	$2^-\mathrm{S}0^+ f_2$ $2^-\mathrm{D}0^+\ \varepsilon$ $2^-\mathrm{D}0^+\ f_2$ $2^-\mathrm{P}0^+\ \rho_3$ $2^-\mathrm{P}0^+\ \rho$ $2^-\mathrm{F}0^+\ \rho$ $2^-\mathrm{D}0^+\ f_0$ $2^-\mathrm{S}1^+ f_2$ $2^-\mathrm{D}1^+\ \varepsilon$ $2^-\mathrm{D}1^+\ f_2$ $2^-\mathrm{P}1^+\ \rho$ $2^-\mathrm{F}1^+\ \rho$ $2^-\mathrm{S}1^- f_2$
$\mathbf{2^+}$	$2^+\mathrm{D}1^+\ \rho$ $2^+\mathrm{P}1^+\ f_2$ $2^+\mathrm{D}0^-\ \rho$ $2^+\mathrm{D}1^-\ \rho$
$\mathbf{3^+}$	$3^+\mathrm{S}0^+\ \rho_3$ $3^+\mathrm{P}0^+ f_2$ $3^+\mathrm{D}0^+\ \rho$ $3^+\mathrm{F}0^+\ \varepsilon$ $3^+\mathrm{D}1^+\ \rho$
$\mathbf{4^-}$	$4^-\mathrm{F}0^+\ \rho$
$\mathbf{4^+}$	$4^+\mathrm{F}1^+ f_2$ $4^+\mathrm{G}1^+\ \rho$

PWA with full rank ρ. Maximum LK method

$$\ln \mathcal{L} = \sum_{e=1}^{N_{ev}} \ln \sum_{i,j=1}^{N_w} C_{k(i)} R_{m(i)m(j)} C^*_{k(j)} \mathcal{M}_i(\tau_e) \mathcal{M}^*_j(\tau_e)$$

$$- \quad N_{ev} \sum_{i,j=1}^{N_w} C_{k(i)} R_{m(i)m(j)} C^*_{k(j)} \int \varepsilon(\tau) \mathcal{M}_i(\tau) \mathcal{M}^*_j(\tau)\, d\tau$$

- N_{ev} — number of events, N_w — number of waves
- $\mathcal{M}(\tau_e)$ — amplitudes for e-th event (data)
- R — positive definite density matrix (parameters)
- C — coupling coefficients, constants)
- $m(i)$, $k(i)$ — describes wave to C and R correspondence
- $\tau = s, t, m(3\pi), \ldots$ — phase space variables
- $\varepsilon(\tau)$ — acceptance of the setup

PWA with rank one ρ. Maximum LK method

$$\ln\mathcal{L} = \sum_{e=1}^{N_{ev}} \ln \sum_{i,j=1}^{N_w} C_{k(i)}C^*_{k(j)}\mathcal{M}_i(\tau_e)\mathcal{M}^*_j(\tau_e)$$

$$- \quad N_{ev}\sum_{i,j=1}^{N_w} C_{k(i)}C^*_{k(j)}\int \varepsilon(\tau)\mathcal{M}_i(\tau)\mathcal{M}^*_j(\tau)\,d\tau$$

- N_{ev} — number of events, N_w — number of waves
- $\mathcal{M}(\tau_e)$ — amplitudes for e-th event (data)
- C — coupling coefficients (parameters)
- $k(i)$ — describes wave to C correspondence
- $\tau = s, t, m(3\pi), \ldots$ — phase space variables
- $\varepsilon(\tau)$ — acceptance of the setup

Coherent part of density matrix

Coherent part of the density matrix R is the largest part of the matrix which has rank 1 and behaves like vector of amplitudes. Let

$$R = \sum_{k=1}^{d} e_k * V_k * V_k^+ \quad \text{where} \quad \begin{cases} e_k \text{ is k-}th \text{ eigenvalue} \\ V_k \text{ is k-}th \text{ eigenvector} \end{cases}$$

Let $e_1 \gg e_2 > \ldots > e_d > 0$. Now

$$R = R_L + R_S, \quad R_L = e_1 * V_1 * V_1^+, \quad R_S = \sum_{k=2}^{d} e_k * V_k * V_k^+$$

Part R_L corresponds to largest eigenvalue (LEV) of R (coherent part of R) while R_S is the rest, incoherent part of R. This decomposition is stable w.r.t. variations of R matrix elements. Experience shows that resonances tend to concentrate in R_L.